ELSEVIER

Journal of Hydrology 267 (2002) 217–226

Journal of Hydrology

www.elsevier.com/locate/jhydrol

Analyses of soil water content variations and GPR attribute distributions

B. Schmalz[a,1], B. Lennartz[b,*], D. Wachsmuth[c,2]

[a]*Institute of Water Management and Landscape Ecology, University Kiel, Olshausenstr. 40, D-24118 Kiel, Germany*
[b]*Institute of Soil Science, University Rostock, Justus-von-Liebig-Weg 6, D-18051 Rostock, Germany*
[c]*Institute of Geosciences, Geophysical Section, University Kiel, Otto-Hahn-Platz 1, D-24118 Kiel, Germany*

Abstract

Water flux was investigated in the frame of the project 'preferential flow paths—3D water and solute dynamic in heterogeneous media'. The objective of the study was the non-destructive three-dimensional monitoring and description of heterogeneous flux fields with hydrological and geophysical methods. A large tank filled with homogeneous sand was set up to realize infiltration experiments. We compared the parameter distribution calculated from measurements of a ground penetrating radar system (GPR) with a simulated water content distribution using a two-dimensional numerical model based on the Van Genuchten–Mualem approach in order to assess the effectiveness of the geophysical measure for the characterization of soil water content variations. A statistical examination of both simulated water contents based on independent measured soil properties and reflection amplitudes from radargrams indicated a better conformity between geophysical data and simulated water contents assuming a heterogeneous hydraulic parameter distribution. The heterogeneous nature of the sand body could be confirmed by dye tracer experiments. The analyzed GPR attribute, the distribution of the maximum reflection amplitudes, may serve in future studies as an indicator for the expected water content heterogeneity in sandy soils. © 2002 Published by Elsevier Science B.V.

Keywords: Ground penetrating radar; Flux field; Variability; Soil water content

1. Introduction

In many studies, the importance of small scale variations in water content on the heterogeneity of the flux field and the generation on preferential flow paths has been documented (Roth et al., 1991; Schuh et al., 1993; Mallants et al., 1997). The estimation of spatial distributions of soil water content is not bound only to hydrological methods, but can also be realized by geophysical measurements especially when a non-destructive method is required. Ground penetrating radar (GPR) provides high resolution images of near-surface sedimentary packages. With respect to water content variability analysis, two different procedures based on GPR measurements can be distinguished.

Various authors use tomographic or multi-offset radar methods to determine the velocity of an electromagnetic wave through the subsurface. The dielectric constant can be calculated approximately from the velocity. Water content is then usually derived from the dielectric constant using the popular empirical Topp equation (Topp et al., 1980) or mixture formulae (i.e. Roth et al., 1990) which describe the relationships between dielectric and

* Corresponding author. Fax: +49-381-498-2159.
E-mail addresses: bernd.lennartz@auf.uni-rostock.de (B. Lennartz), britta.schmalz@web.de (B. Schmalz), dwachsmuth@geophysik.uni-kiel.de (D. Wachsmuth).
[1] Fax: +49-431-880-4083.
[2] Fax: +49-431-880-4432.

0022-1694/02/$ - see front matter © 2002 Published by Elsevier Science B.V.
PII: S0022-1694(02)00152-X

hydraulic parameters. Using this procedure, Hubbard et al. (1997), Parkin et al. (2000), Greaves et al. (1996) and Sénéchal et al. (2000a) investigated the use of radar data for estimating subsurface water content.

Another method of estimating water content distributions from GPR data is to look for a variable which statistically or geostatistically describes this distribution. In this case, the analysis of radar data is used for characterizing the heterogeneity of the subsurface. To calculate any kind of distribution from radar data, the recorded radar traces are analyzed using different attributes. This method is analogous to seismic trace analyses. Chen and Sidney (1997) gave an overview of seismic attributes which are specific measurements of geometric, kinematics, dynamic, or statistical features derived from the recorded data. Using this procedure for electromagnetic applications, Sénéchal et al. (2000b) gave a complex interpretation of a 3D GPR data set using attributes calculated from amplitude analysis of reflected radar waves. They developed an understanding of the lateral continuities and discontinuities of the reflectors, the geometry of structures and their dynamic characteristics. Knight et al. (1997) used the amplitude values recorded in the radar traces for a geostatistical analysis of the GPR data. The spatial variation in dielectric properties in the subsurface was closely related to the spatial variation in grain size. The geostatistical analysis captured information about the spatial distribution of the dominant sedimentological features. Rea and Knight (1998) found an excellent agreement using geostatistical analysis of a digitized photograph and the radar data (amplitudes). The GPR data did image the spatial distribution of lithologies and could be used to quantify the correlation structure of the sedimentary unit. They also observed a good agreement between the spatial variation in dielectric properties in the subsurface and the spatial variation of the grain size both indicating the heterogeneity of the subsurface. The authors hypothesized that information extracted from the GPR data can be used to describe spatial variability of hydraulic properties. Also Tercier et al. (2000) found that geostatistical analysis of GPR data gave an effective way of quantifying the correlation structure of the two-dimensional GPR image. Charlton (2000) used GPR techniques for spatially distributed measurements of volumetric soil moisture. He found significant relationships between maximum amplitude and moisture content, indicating the potential of GPR for a quantitative assessment of soil moisture at different depths.

The aim of this study was to assess the heterogeneity of a sand body and the resulting water content distribution by GPR and soil hydraulic modeling. The distribution of hydraulic parameters (e.g. water content) can be assessed from geophysical measures only if there is a relationship between attributes (amplitudes, frequency content) of the radar traces and hydraulic parameters. Most attributes may not allow a quantitative analysis of the hydrological properties, but may be useful in defining their variation which on its part could be of great use, for instance, for characterizing the vulnerability of soil–water systems to preferential flow. One possible attribute is the reflection amplitude in a radargram which was used in this study as a parameter to be compared to the water content.

2. Materials and methods

2.1. Experimental set-up

In order to realize infiltration experiments, a large physical sand model (base 5 m × 3 m; surface 6 m × 5.6 m) with three sloped side walls was constructed and filled with 2 m homogeneous sand (Hagrey et al., 1999; Fig. 1). Measurements of water tension, water content (using time domain reflectometry (TDR)) and GPR data have been carried out. While the radar system yields two-dimensional images of the irrigated center part of the sand tank, the tensiometer and TDR probes allowed only the registration of the soil hydraulic parameters at one location in eight depths. The lower boundary was constructed for a spatial resoluted discharge registration. An irrigation system allowed the adjustment of different infiltration intensities on the central part of the surface area. The irrigation device consisted of a mobile spray bar with eight nozzles, which was moved evenly over the sand surface and enabled a uniform and continuous irrigation. Ten realized infiltration experiments, from which we considered one in this study, revealed the non-uniform discharge behavior of the sand tank. In the selected experiment a

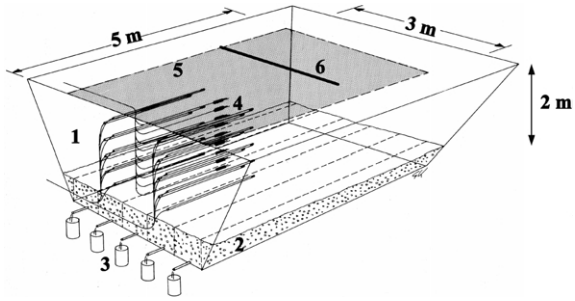

Fig. 1. Experimental set-up of the sand tank: (1) sand; (2) drainage layer (gravel); (3) discharge registration; (4) tensiometers; TDR-sensors; (5) irrigated area; (6) GPR profile.

continuous irrigation of 4300 l (287 mm) in 14 h, produced a discharge of 3154 l (197 mm) over an observation period of 14 days. The experimental study was finalized with a dye tracer test to visualize flow patterns. The dye (Vitasyn Blau AE85) was applied (50 mm; 4 g/l) over a subarea of 4 m^2 and afterwards excavated layer-wise (20 cm) horizontally.

2.2. Water content distributions

Numerical experiments with the software package 'HYDRUS-2D' (Simunek et al., 1996) were conducted to obtain two-dimensional views of water flow under various unsaturated flow scenarios (Van Genuchten–Mualem approach). The program includes the two-dimensional finite element model SWMS-2D (Simunek et al., 1994) and numerically solves the Richards' equation for water flow. The soil hydraulic functions were derived from water tension and content data measured in situ during the infiltration experiments (Van Genuchten et al., 1991). The saturated hydraulic conductivity was calculated (Hazen equation; Hölting, 1996) from the grain size distribution of the sand which was investigated at 112 locations in various depths.

The two flow scenarios presented in this study were generated:

(i) by using one representative individual water retention curve (from 60 cm soil depth) of the eight measure depths in order to obtain a homogeneous soil profile and
(ii) by randomly distributing the measured hydraulic functions (as estimated in eight depths) over the entire numerical mesh aiming at setting up a heterogeneous case.

From measurements on bulk density and grain size distribution in ten and two depths, respectively, with 25–30 samples per depth no spatial autocorrelation of the investigated parameters was observed. Accordingly, the heterogeneous case was established, assuming the hydraulic properties to be spatially independent.

The results from the destructive dye tracer test showed fingerlike flow patterns and indicated a heterogeneous flux field (Fig. 2). This observation, as a qualitative indicator of the flow regime, supported the need to use a heterogeneous numerical model.

The simulated spatial variability of water content in different depths at various time steps was investigated by statistical analysis and box-whisker-plots. The latter give median, range, quartile, outliers and extrema of a distribution. For a reasonable comparison with the results of GPR measurements, only the central part of the sand tank was taken into consideration.

2.3. Geophysical experiments

To track the water movement during the infiltration experiments several GPR profiles were acquired at varying locations. In some experiments only one or two profiles were recorded, while during others up to 15 parallel profiles with a spacing of 10 cm were registered to get a more detailed picture in three dimensions. All measurements were repeated in time steps of about 15–20 min when only one or two profiles, and of 30 min when 15 parallel profiles were recorded. The chosen time resolution resulted from technical constraints. For all measurements, the Subsurface–Interface–Radar-10A-System (SIR 10A) of Geophysical Survey Systems Inc. (GSSI) with one or two 500 MHz antennas was used. Each antenna unit consisted of a shielded transmitter and a shielded receiver antenna with a spacing of 30 cm. All measurements were performed in bistatic mode. To get an accurate positioning during the infiltration experiments, the antennas were mounted on the irrigation device, which moved over the sand body with constant velocity. Parallel profile positioning was realized using fixed patterns, so

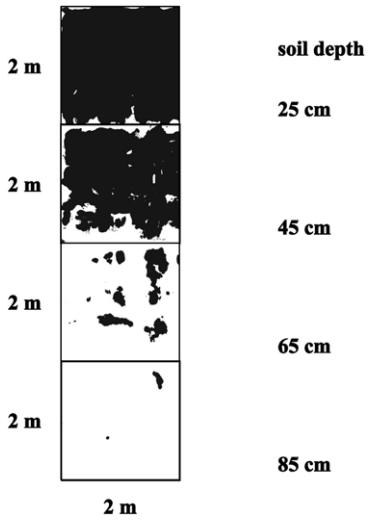

Fig. 2. Four soil layers with stained flow paths as resulting from the application of 50 mm dye solution. The proportion of the conducting flow region, expressed as dye coverage, decreases with depth.

that all time-dependent measurements originated exactly from the same position. The altitude of the antennas over ground was 10 cm, which is uncritical for the GPR signal as tests have shown during data-acquisition for a first time-lapse 3D experiment in our sand model (Trinks et al., 2001) which was conducted according to the Borden experiment (Brewster and Annan, 1994; Brewster et al., 1995). Resolution in vertical direction is limited by the wavelength λ of the electromagnetic waves which is a direct function of the center frequency of the antennas f and the propagation velocity v ($\lambda = v/f$). Two reflectors can be distinguished, if the distance exceeds $\lambda/2$. Accordingly, in our experiment a vertical resolution of approximate 10 cm for a wet sand was determined. Horizontal resolution is affected by antenna size and frequency and as the vertical resolution linked to the wavelength; mathematically this can be described through the Fresnel equation. For our configuration the lateral resolution is nearly the same as the vertical in the upper part of the model with decreasing resolution with increasing depth (because of physical reasons related to the Fresnel equation; for details see Daniels (1996)). Because of the fast movement of the water front through the sand body during the infiltration experiments and the need to obtain time-dependent measurements in order to monitor the infiltration process, only constant offset measurements were performed and thereby no multi-offset-processing was possible. As a direct consequence, no velocity model could be calculated from common midpoint (CMP) sections by semblance analysis and converted to water content distributions using, for example, the Topp equation as some authors did before (Greaves et al., 1996). It has to be pointed out, that no available measurement device allows the registration of multi-offset data in time intervals such as they would have been necessary in this study ($<1-3$ min).

The processing steps applied to the acquired GPR data were first counting back the applied field gain curve, then normalizing in space to 1 cm trace-intervals and afterwards reapplying a realistic gain curve taking the attenuation of electromagnetic waves in a mid-electroconductive environment into account. Only a low-cut filter was applied during acquisition for signal stability.

In order to obtain depth profiles, the GPR signal originally acquired in the time domain has to be converted to a depth section. This procedure called ‘migration’ is a common process in seismic data processing. During the migration the data is not simply rescaled, but e.g. effects of the acquisition in the time-domain such as diffraction hyperbolas at edges or isolated bodies are taken into analysis. In this case, a classic Stolt-migration-algorithm was used to convert the time section into a depth section (Stolt, 1978). The procedure is based on a basic velocity model which could not be computed directly from the acquired data base (described earlier). However, from the independent TDR measurements in eight depths it was possible to set up a bedded velocity model neglecting strong variations in the horizontal plane. Some artifacts may be introduced using such a simplified model, but these are uncritical compared with analysis on those arising from time-domain data.

Comparison of water content and GPR attribute was realized on the basis of the descriptive statistics of both measures. Two radargrams recorded at two time steps during the infiltration experiment described earlier were analyzed. At the depth intervals that were also considered for the hydrological analysis, the maximum reflection amplitudes as a possible attribute normalized with the maximum observed value in the interval were plotted.

3. Results

3.1. Soil water content

Various simulation runs showed that the observed variability of discharge in the sand tank was caused by the geometry of the tank and the distribution of soil hydraulic properties. Both effects generated a non-uniform water flux so that a heterogeneous spatial distribution of water content can be assumed.

For comparison purposes two time steps 3 and 13 h after onset of irrigation were chosen. These time steps were considered exemplary for showing the different conditions at the beginning and at the end of the irrigation period. At early stages of the test only the upper part of the sand tank was wetted (Fig. 3(a) and (b)) while the simulation runs indicated a volumetric water content of nearly 0.20 $cm^3\ cm^{-3}$ throughout the soil profile at later stages (Fig. 4(a) and (b)). The two-dimensional cross-sections showed large water contents in the center zone and at the lower boundary of the sand tank and dry lateral areas. The observed general water distribution was caused by the irrigation area which covered only the central part of the model surface. The sloped side walls generated a funnel-like flow behavior which resulted in an increased water content at the lower boundary. In contrast to the homogeneous flow scenario, the simulations with a stochastic distribution of soil hydraulic properties generated, as expected, random structures of water content (Fig. 4(b)).

Box plots of water content within one layer indicated a non-normal distribution for the homogeneous case (Figs. 3(a) and 4(a)) which is mainly related to the non-irrigated dry lateral areas and a nearly normal distribution for the heterogeneous soil profile (Figs. 3(b) and 4(b)). The coefficient of variance for the water content resulting from the homogeneous soil was small compared with the values obtained from generated profiles with random distributions of soil hydraulic parameters (Table 1).

3.2. GPR signals

First, the general suitability of the maximum reflection amplitude as an indicator for the water content variation and thereby of the variability of the hydraulic functions was tested in a numerical experiment. As follows from theory of propagation of electromagnetic waves at the interface of two adjoining materials with different dielectric and electric properties a reflection will occur. The strength of the reflection depends on the difference of the material properties, mainly contrast in dielectricity, which can be calculated by the well-known reflection coefficient R. Fig. 5 shows one example from the numerical experiments, where we considered the hypothetical case of a two layered porous medium. The water content of the second layer was varied at increments of 5 vol.% (properties identifier '0') over a range from 5 vol.% ('0') to 40 vol.% (properties identifier '7'). For all possible combinations of water contents the maximum reflection amplitudes as shown in Fig. 5 were selected from the synthetic radargram calculated using an accurate finite difference modeling code for electromagnetic wave propagation in dispersive media written by Bergmann et al. (1998). Input for each layer were the dielectric permittivity and electric conductivity. Dielectric permittivity was calculated backwards from the given water content using the Topp equation, while electric conductivity was approximated by using the Archie equation (Archie, 1942). The center frequency of the modeled electromagnetic wave was chosen as 500 MHz to match the experimental data. This procedure has been carried out for all other combinations possible in a two-layered soil. From the graphical presentation of all picked maximal reflection amplitudes in Fig. 6, it is obvious that the signal increases along with the increase in water content differences demonstrating the usefulness of the attribute for soil water distribution analysis. For a multi-layered soil as in our sand model there can be two main difficulties in analyzing the amplitude distributions: (i) multiple reflections. In Fig. 5 it can be noticed, that behind the main reflection space multiple reflections occur. From Fig. 5 it is obvious that the amplitudes of these multiple reflections are very small in contrast to the main reflections. If these are a problem in the data, a prediction filter must be applied or the multiples must be filtered, e.g. in the τp-domain. (ii) If there are very large lateral differences in the dielectric properties of a profile, analyses may be incorrect. Given that a soil layer is partly overlaid by highly attenuating material, the resulting distribution may show a hard contrast of low and high reflection amplitudes. Such phenomena can

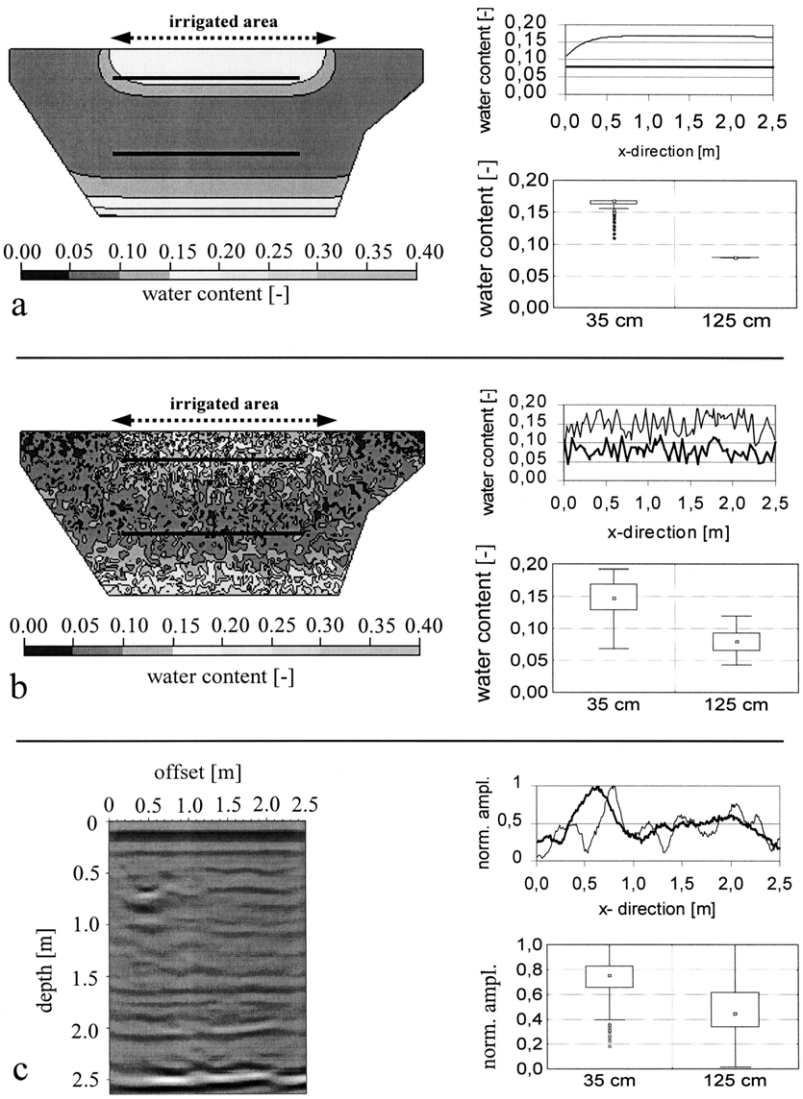

Fig. 3. (a) Simulated water flux in a homogeneous soil profile 3 h after onset of irrigation. (b) Simulated water flux in a soil with a random distribution of soil hydraulic parameters 3 h after onset of irrigation: two-dimensional distribution of water content (left) with selected profiles at depths of 35 and 125 cm (black lines), water content distribution within one layer (right, top) at two depths: 35 cm (thin line) and 125 cm (thick line), box plots of water content distribution within one layer (right, bottom) at different depths: 35 and 125 cm. (c) Migrated radargram 3 h after onset of irrigation (left), distribution of normalized amplitudes (right, top) at two depth intervals: 30–40 cm (thin line) and 120–130 cm (thick line), box plots of normalized amplitudes distribution (right, bottom) at different depths: 35 and 125 cm.

be neglected for our rather homogeneous sand material.

The processed GPR profiles (prior migration) allowed the clear identification of the penetrating water front in the considered infiltration experiment especially when difference radargrams of two subsequent time steps were computed (Fig. 7(a) and (b)). Difference radargrams are generated by directly subtracting the corresponding amplitudes of all radar traces (250 per time step) from the two treated time steps. The result of such a computation must be read from top to the lower limit. Regions that appear rather uniform are unchanged from time step to time step. In contrast, certain reflection patterns (A in Fig. 7) have

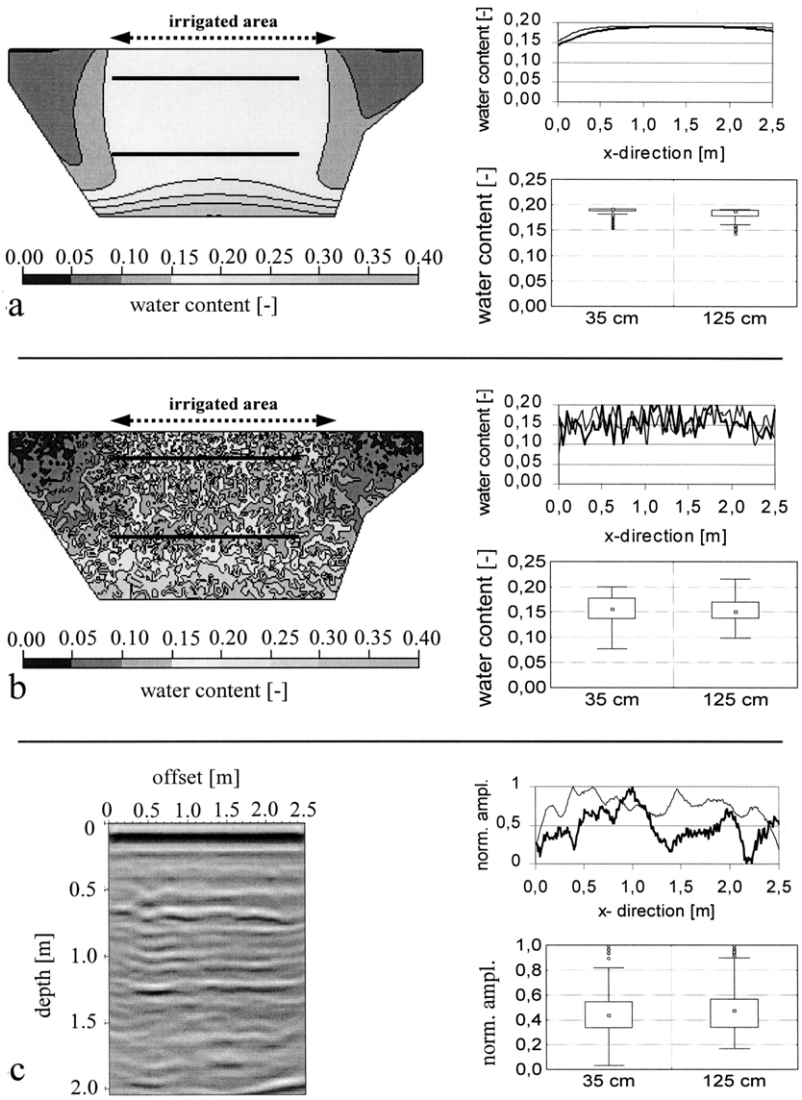

Fig. 4. (a) Simulation of water flux in a homogeneous soil 13 h after onset of irrigation. (b) Simulation of water flux in a soil with a random distribution of soil hydraulic parameters 13 h after onset of irrigation: two-dimensional distribution of water content (left) with selected profiles at depths of 35 and 125 cm (black lines), water content distribution (right, top) at two depths: 35 cm (thin line) and 125 cm (thick line), box plots of water content distribution (right, bottom) at different depths: 35 and 125 cm. (c) Migrated radargram 13 h after onset of irrigation (left), distribution of normalized amplitudes (right, top) at two depth intervals: 30–40 cm (thin line) and 120–130 cm (thick line), box plots of normalized amplitudes distribution (right, bottom) at different depths: 35 and 125 cm.

changed with time, indicating the moving water front. Most of the visible reflections are artifacts or altered characteristics of very dominant reflections (e.g. concrete base of sand tank).

The migrated radargram showed the construction basis of the sand tank (concrete) at 2.50 m (Fig. 3(c)). Furthermore, a layered structure of the sand became visible which was possible due to the filling procedure of the tank (layer-wise filling and compaction). The variability within one layer was visualized by the normalized amplitudes plotted in Figs. 3(c) and 4(c).

The box plots of the amplitudes (Figs. 3(c) and 4(c)) showed a normal distribution which is not in line with the hydrological simulation results assuming a

Table 1
Descriptive statistics of water content and normalized GPR amplitudes 3 and 13 h after onset of irrigation in a depth of 35 and 125 cm

	Hours after onset of irrigation	Homogeneous		Heterogeneous		GPR	
Depth (cm)		35	125	35	125	35	125
n		134	103	134	102	250	250
Mean	3	0.16 $m^3 m^{-3}$	0.08 $m^3 m^{-3}$	0.15 $m^3 m^{-3}$	0.08 $m^3 m^{-3}$	0.74	0.48
CV	3	0.07	0.00	0.18	0.25	0.20	0.43
Mean	13	0.19 $m^3 m^{-3}$	0.18 $m^3 m^{-3}$	0.16 $m^3 m^{-3}$	0.16 $m^3 m^{-3}$	0.44	0.49
CV	13	0.04	0.06	0.17	0.18	00.45	0.39

n is the number of samples, CV is the coefficient of variation.

homogeneous soil. A better agreement between the distributions of the simulated water content and of the amplitudes can be observed for the heterogeneous soil profile. The amplitude distribution had in general a higher coefficient of variance than the simulated water content distribution indicating that the GPR signal accounts for more than just water content differences. Differences in CVs might show that the maximum reflection amplitude is an integrative signal accounting for several soil physical properties which on their part determine water content distributions (Table 1).

4. Conclusions

There is a relationship between soil hydraulic properties and the amplitudes in the radargram. An analysis of the measured GPR data and dye tracer test gave an indication about heterogeneities of the sand and resulting water content distributions. Although water content can be derived from GPR velocities in general, a direct derivation of water content from GPR amplitudes is not possible especially under field-like conditions with structured soils.

Statistical analyses of certain coefficients and parameters obtainable from the GPR measurements might be a way to reveal the heterogeneity of the soil water content and the related flux field. First results presented in this study indicated that the assumption of a heterogeneous distribution of soil hydraulic properties coincides better with the geophysical data than a generated homogeneous case. It can be concluded that even in homogeneous sand profiles local variabilities dominate water flow which

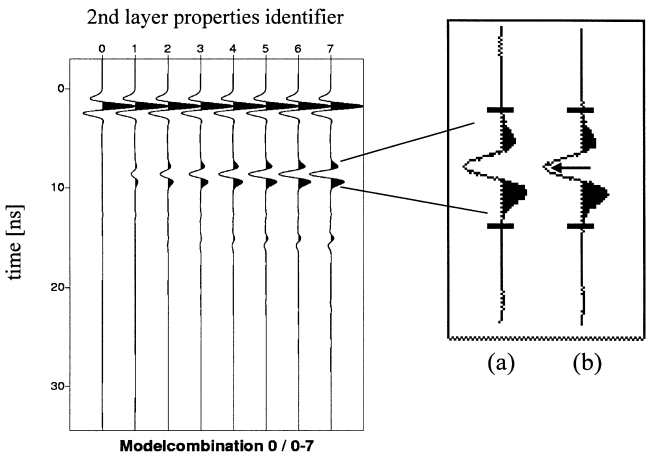

Fig. 5. Results of numerical GPR-simulations of a two-layered soil (left; layer properties identifier: 0 = 5 vol.%,…,7 = 40 vol.% water content): First layer was held constant while the second one changed from 5 to 40 vol.% in steps of 5 vol.% in water content. The first reflection from the top is the direct wave, while the second indicates the different reflection amplitudes with changing water content. The third rather small reflection is a multiple of the second. Right: computing the maximal reflection amplitude attribute; first an interval of interest is selected (a), then the absolute value of the maximal amplitude is taken for further analysis (b).

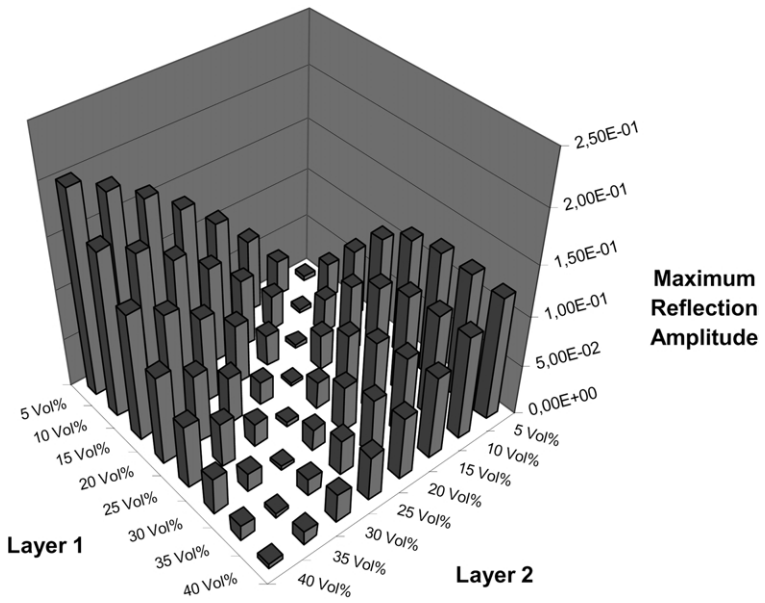

Fig. 6. Effect of water content combinations in a layered sandy soil on the absolute value of the maximum reflection amplitude. Except for a homogeneous soil (same parameter set for layer 1 and layer 2) the amplitude varies significantly with water content differences in the two considered layers.

confirms other studies in which for instance the dye tracer technique have been used to identity flow patterns (Flury et al., 1994). The variances of the soil hydraulic and geophysical parameters differed although in general the heterogeneous case performed better than the homogeneous.

The next step essential for evaluating the potential of the method would be using the analyzed variance of GPR amplitudes for each depth interval directly in the numerical models for simulating water flow. We expect a better description of the water flux variation by using the information about soil heterogeneity derived from GPR measurements. Comparisons of discharge rates derived from numerical models based on soil hydraulic parameter distributions determined from the GPR analysis with real measured data, will

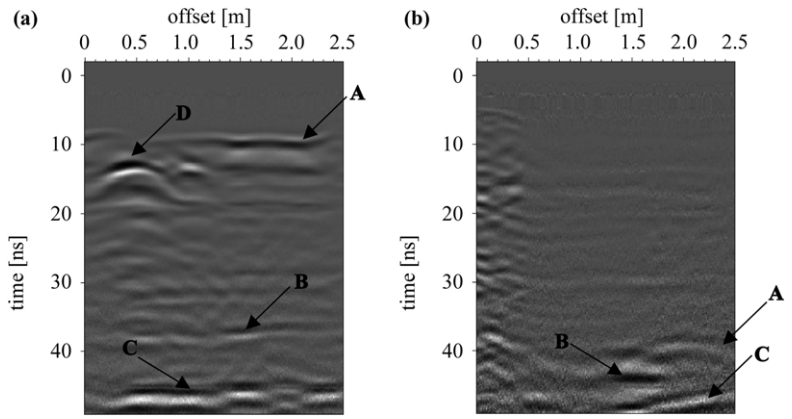

Fig. 7. Difference radargrams (non-migrated) of the radargrams (a) 3 and 2.45 h and (b) 13 and 12.43 h after onset of irrigation. (A) marks the water front, (B) the electrode grid in 2 m depth, (C) the concrete bottom in 2.5 m depth and (D) is a highlighted artifact of a diffraction hyperbola caused by an electrode for geoelectric measurements not reported in this paper.

show if a better agreement of model predictions and experimental results can be achieved.

References

Archie, G.E., 1942. Electrical resistivity log as an aid in determining some reservoir characteristics. Trans. AIME 146, 54–62.

Bergmann, T., Robertsson, J.O.A., Holliger, K., 1998. Finite-difference modeling of electromagnetic wave propagation in dispersive and attenuating media. Geophysics 63 (3), 856–867.

Brewster, M.L., Annan, A.P., 1994. Ground-penetrating radar monitoring of a controlled DNAPL release: 200 MHz radar. Geophysics 59 (8), 1211–1221.

Brewster, M.L., Annan, A.P., Greenhouse, J.P., Kueper, B.H., Olhoeft, G.R., Reman, J.D., Sander, K.A., 1995. Observed migration of a controlled DNAPL release by geophysical methods. Ground Water 33 (6), 977–987.

Charlton, M., 2000. Small scale soil-moisture variability estimated using ground penetrating radar. Extended abstract. In: Proceedings of the Eighth International Conference on Ground Penetrating Radar, Gold Coast, Australia, 23–26 May.

Chen, Q., Sidney, S., 1997. Seismic attribute technology for reservoir forecasting and monitoring. The Leading Edge, 445–456.

Daniels, D.J., 1996. Surface-penetrating Radar, The Institution of Electrical Engineers; Radar, Sonar, Navigation And Avionics Series 6, Short Run Press, Exeter, UK.

Flury, M., Flühler, H., Jury, W.A., Leuenberger, J., 1994. Susceptibility of soils to preferential flow of water: a field study. Water Resour. Res. 30, 1945–1954.

Greaves, R.J., Lesmes, D.P., Lee, J.M., Toksöz, M.N., 1996. Velocity variations and water content estimated from multi-offset, ground-penetrating radar. Geophysics 61 (3), 683–695.

Hagrey, S.Aal., Schubert-Klempnauer, T., Wachsmuth, D., Michaelsen, J., Meissner, R., 1999. Preferential flow: first results of a full-scale flow model. Geophys. J. Int. 138, 643–654.

Hölting, B., 1996. Hydrogeologie. Einführung in die allgemeine und angewandte Hydrogeologie, Enke, Stuttgart, p. 441.

Hubbard, S.S., Peterson, J.E., Majer, E.L., Zawislanski, P.T., Williams, K.H., Roberts, J., Wobber, F., 1997. Estimation of permeable pathways and water content using tomographic radar data. The Leading Edge, 1623–1628.

Knight, R., Tercier, P., Jol, H., 1997. The role of ground penetrating radar and geostatistics in reservoir description. The Leading Edge, 1576–1582.

Mallants, D., Mohanty, B.P., Vervoort, A., Feyen, J., 1997. Spatial analysis of saturated hydraulic conductivity in a soil with macropores. Soil Technol. 10, 115–131.

Parkin, G., Redman, D., Von Bertoldi, P., Zhang, Z., 2000. Measurement of soil water content below a wastewater trench using ground-penetrating radar. Water Resour. Res. 36 (8), 2147–2154.

Rea, J., Knight, R., 1998. Geostatistical analysis of ground-penetrating radar data: a means of describing spatial variation in the subsurface. Water Resour. Res. 34 (3), 329–339.

Roth, K., Schulin, R., Flühler, H., Attinger, W., 1990. Calibration of time domain reflectometry for water content measurement using a composite dielectric approach. Water Resour. Res. 26 (10), 2267–2273.

Roth, K., Jury, W., Flühler, H., Attinger, W., 1991. Transport of chloride through an unsaturated field soil. Water Resour. Res. 27, 2533–2541.

Schuh, W.M., Meyer, R.F., Sweeney, M.D., Gardner, J.C., 1993. Spatial variation of root-zone and shallow vadose-zone drainage on a loamy glacial till in a sub-humid climate. J. Hydrol. 148, 1–26.

Sénéchal, P., Perroud, H., Garambios, S., 2000a. Geometrical and physical parameters comparison between GPR data and other geophysical data. Extended abstract. In: Proceedings of the Eighth International Conference on Ground Penetrating Radar, Gold Coast, Australia, 23–26 May.

Sénéchal, P., Perroud, H., Sénéchal, G., 2000b. Interpretation of reflection attributes in a 3-D GPR survey at Vallée d'Ossau, western Pyrenees, France. Geophysics 65 (5), 1435–1445.

Simunek, J., Vogel, T., Van Genuchten, M.Th., 1994. The SWMS-2D code for simulating water flow and solute transport in two-dimensional variably saturated media. Research Report No. 132. US Salinity Lab., USDA/ARS, Riverside, CA.

Simunek, J., Sejna, M., Van Genuchten, M.Th., 1996. Hydrus-2D, Simulating water flow and solute transport in two-dimensional variably saturated media. User's Manual. US Salinity Lab., USDA/ARS, Riverside, CA.

Stolt, R.H., 1978. Migration by Fourier transform. Geophys. Soc. Expl. Geophys. 43, 23–48.

Tercier, P., Knight, R., Jol, H., 2000. A comparison of the correlation structure in GPR images of deltaic and barrier-spit depositional environments. Geophysics 65 (4), 1142–1153.

Topp, G.C., Davis, J.L., Annan, A.P., 1980. Electromagnetic determination of soil water content. Measurements in coaxial transmission lines. Water Resour. Res. 16, 572–582.

Trinks, I., Wachsmuth, D., Stümpel, H., 2001. Monitoring water flow in the unsaturated zone using georadar. First Break 19 (12), 679–684.

Van Genuchten, M.Th., Leij, F.J., Yates, S.R., 1991. The RETC code for quantifying the hydraulic functions of unsaturated soils. US Salinity Lab., USDA/ARS, Riverside, CA.